Advanced spatial adaptive channel estimation for efficient mmWave communication

Rajkumar M. Vadgave, Manjula S.
Department of Electronics and Communication Engineering, Bheemanna Khandre Institute of Technology, Bhalki, India

Article Info

ABSTRACT

This study explores the intricacies posed by the unique features of 5G/6G wireless sensor networks (WSNs) to guarantee dependable and long-lasting connectivity. The increasing energy consumption in 5G/6G networks due to higher data rates and more complex architectures emphasizes the necessity for energy-efficient techniques. The WSN resources are limited, specially designed resource allocation and management techniques are essential. In this paper, a unique analogue combining design called advanced spatial adaptive channel estimation (ASACE) and an optimization model for channel state information (CSI) estimation that takes use of the low-rank characteristics of channel matrix sparsity are presented. Gradient descent (GD) optimization is incorporated to improve the suggested approach, demonstrating improvements in residual errors and computing complexity. The optimization problem aims to find the gains and orientations of wideband channel paths. Moreover, a comparative analysis is conducted between the suggested model and many cutting-edge methods, emphasizing error minimization. This thorough analysis offers a nuanced viewpoint on the effectiveness and efficiency of the suggested ASACE approach in the context of wideband cross-entropy (CE) and optimization, which makes a significant contribution to the area.

Corresponding Author:

Rajkumar M. Vadgave
Department of Electronics and Communication Engineering, Bheemanna Khandre Institute of Technology
Bhalki, India
Email: rajkumarv074@gmail.com

1. INTRODUCTION

The spatial and frequency domain dimensions of wireless signals are expanding quickly to meet the increasing demand for communication capacity in 6G networks [1]. From 5G to 6G, there is a noticeable shift in the spatial domain from massive-multiple-input multiple-output (mMIMO) to very large-scale MIMO (XLMIMO) and XL-MIMO increases spectral efficiency tenfold with a notably higher number of antennas [2]. In order to access greater spectrum resources, the operational frequency simultaneously moves from sub-6G to the terahertz (THz) and millimeter wave (mmWave) bands [3]. Many high-gain arrays at high frequencies have been designed as a result of the smaller wavelength, which causes high-frequency antennas to be proportionately smaller in size [4], [5]. Therefore, it is natural and acknowledged that XL-MIMO and high-frequency communications are essential technologies for the development of 6G communications. Like 5G mmWave massive MIMO, high-frequency communications use hybrid precoding to reduce radio-frequency (RF) chain power consumption [6], and accurate channel state information (CSI) is essential for successful hybrid precoding. Intelligent communication systems, large data platforms, and advanced processing applications all require the integration of wireless communication technology. This integration is expected to be more thorough in the world of 6G technology, expanding on the foundation established by 5G

technologies and the 6G networks are designed to support interactive media, mapping, and high-speed phone services [7], [8]. Wireless sensor networks (WSNs) are crucial for 5G and 6G networks, which aim to provide fast, reliable, and comprehensive connections for various devices and applications.

Enhanced data throughput, lower latency, wide device connectivity, and network slicing will boost wireless communication. WSNs can leverage 5G/6G infrastructure for better long-distance communication and network integration. However, 5G/6G's high data rates and complexity pose challenges for WSNs, which have limited memory, CPU, power, and network throughput. Energy-efficient techniques and optimized algorithms are necessary to ensure long-term, sustainable communication, addressing WSNs' resource constraints through tailored resource allocation and management strategies. In these scenarios, non-orthogonal pilot sequences are used due to many devices and short wireless channel coherence time. The key finding is that user activity sparsity allows for a compressed sensing (CS) approach [9]–[16], where study [9] explores user activity and data detection for code division multiple access (CDMA) systems with perfect CSI at the base station (BS). When CSI is unavailable, [10], [11] jointly address user activity detection and cross-entropy (CE). Xu *et al*. [10] proposes a Bayesian CS technique for cloud radio-access network, while [11] uses basis pursuit denoising for orthogonal frequency division multiplexing (OFDM) systems.

Studies [12], [13] focus on cooperative information decoding using various CS algorithms. However, a major limitation in previous research is the lack of thorough performance analysis for non-orthogonal multiple-access techniques, especially with large connections. To address this, recent work suggests using the approximate message passing (AMP) technique for simultaneous user activity detection and CE [14], [15]. This approach, aided by state evolution analysis [16], simplifies evaluating missed detection and false alarm probabilities. However, the analysis in [14], [15] is complex, particularly with multiple antennas at the BS, and is limited to device detection without considering its impact on user achievable rates. To overcome these issues, Zhang *et al*. [17] introduces a hybrid beamforming (HBF) approach, combining analog beamforming for beam alignment and digital beamforming for effective interference mitigation. Prior research lacks comprehensive performance analysis, especially with many connections and complex antenna configurations, and focuses mainly on device detection without addressing its impact on user rates.

Recognizing constraints in RF chains, this paper introduces an innovative analogue combining design featuring a random spatial sampling arrangement and the design incorporates a purely random stage preceding the input of analogue received signals into the digital component of the HBF receiver. This configuration is employed for gathering channel session measurements, utilizing an analogue combiner with valves to approximate signals at individual receiving antennas. The proposed model, named advanced spatial adaptive channel estimation (ASACE), distinguishes itself with the unique characteristic of randomly selecting analogue receive beams during the channel period. Coupled with the suggested CSI estimation approach, this design enhances performance while requiring shorter training periods.

The matrix produced at the HBF receiver after the analogue processing of training signals with multiple receiving beams exhibits an identical rank to that of the mmWave MIMO channel matrix. Leveraging this observation, we formulate a CSI estimation optimization model that capitalizes on both the low-rank property of channel matrix sparsity and the received training signal matrix in the beamspace. The proposed optimization problem aims to discern the orientations and gains of the wideband channel paths and the distinctions lie in the mathematical formulations. The low-rank feature specific to narrowband mmWave MIMO channels determines their measurement requirements and the scalability of the technique in wideband mmWave MIMO channels. Additionally, we incorporate the gradient descent (GD) optimization approach, contributing to the reduction of residual errors and computational complexity in the proposed methodology. ASACE can be applied to enhance the performance of wideband mmWave MIMO communication systems in various scenarios, including urban environments, IoT networks, and high-speed mobile communication.

2.   LITERATURE SURVEY

Classic least squares (LS) estimators require large pilot overheads due to the limitation on the number of RF chains, as received pilots must match the channel's dimensions for robust estimation. Using past channel knowledge can alleviate this issue. To address this, various CS-based algorithms, categorized into Bayesian, deep learning (DL), and sparse reconstruction methods, have been explored. Sparse reconstruction methods rely on creating a dictionary matrix that represents channel as the sparse vector. The CE then becomes a sparse reconstruction problem, which can be solved using commercial techniques [18]. A discrete Fourier transform (DFT)-based dictionary shows channel sparsity for a uniform array in the far field, equivalent to sampling the angular domain with uniform grids [19]. Angle and distance affect the array response near the array, necessitating specific grid patterns to sample both domains [20]. Studies show that near-field channels cannot be properly sparsified with far-field dictionaries and vice versa [21]. Determining the fraction

of path components is crucial for designing optimal hybrid-field dictionaries, but this remains unresolved. Current literature recommends dictionary learning for non-uniform arrays in hybrid-field mode [22], where a site-specific dataset optimizes the dictionary, though it may not transfer well to other sites. Bayesian techniques rely on the channel's prior distribution, with iterative algorithms like AMP achieving optimal estimation if the prior is known [23].

The true preceding distribution is often unfamiliar in real-world scenarios and to address this, earlier research empirically chose a base distribution and updated its parameters iteratively using the expectation-maximization principle. These priors can be unstructured (e.g., Gaussian mixture [24], Laplacian [25], or Bernoulli-Gaussian [26]) or structured (e.g., hidden Markov model [27]) when detailed channel knowledge is available. Matched and structured priors usually provide more accurate estimations but rely on complex channel models with robust assumptions, which may not be feasible for hybrid-field THz UM-MIMO channels. Unstructured priors can adapt to various channel conditions but might struggle with accuracy. A deep belief network (DBN)-based energy-efficient routing system has been developed to reduce energy consumption and enhance data transmission efficiency [28]. Effective IoT data transfer requires energy-efficient WSN deployment. Although several routing protocols exist, none have achieved optimal speed and efficiency [29]. Implementing 5G/6G solutions is essential for higher data rates and lower latency, with data rates measured in gigabits per second.

Comparing 5G/6G networks with 3G, 4G, and LTE shows significant improvements in BS bandwidth and quality of service (QoS) [30]. Opting for 5G/6G networks enhances QoS, increases capacity, and addresses modern cellular network challenges, aligning with technological advancements and rising multimedia data consumption. These networks interconnect multiple BSs and systems [31]. In standard and attack scenarios, routing algorithms in mobile ad hoc network (MANETs) maintain a consistent packet transmission ratio, lower overhead connections, and shorter end-to-end delays. Compared to other advanced MANET routing protocols, like ad-hoc on-demand distance-vector, these algorithms, especially when combined with an ant colony optimization algorithm based on optimized fuzzy algorithms, are more effective and perform better [32]. To integrate e-health systems into 5G-based WSNs, a study proposed a quick authentication process considering user requests and time constraints. The healthcare system facilitates data storage and communication for e-health users, drawing significant academic interest. However, the rise of wireless devices and sensors raises privacy and security concerns [33]. Researchers explored a game-theoretic zone-based routing protocol to enhance node cooperation and power efficiency. Current research focuses on CE and HBF with AI algorithms, but high computational complexity and power consumption hinder performance. To address this, [34] proposed a deep-network-based HBF for 5G MIMO systems.

3. PROPOSED METHOD

In this work, we examine a point-to-point communication network, denoted as $A_R \times A_T$ large MIMO, operating in wideband mmWave channels and in this scenario, the transmitter is stimulated with A_T antennas, and the receiver has A_R antennas. Our assumption is that each of the A_T antenna components of the transmitter is connected to an individual RF chain and, the receiver's antenna is linked to A_R, which is less than N_R at RF chains. This configuration allows the transmitter to digitally precode up to A_T distinct signals from a single dedicated RF link. Additionally, we consider the receiver to be equipped with the HBF designs [35], enabling both digital and analog combining. The mmWave MIMO network under consideration involves a wireless communication link for information $b_c \leq \min(A_T, A_R)$, which is separate from the data streams.

An analog-based HBF-receiver for wideband MIMO channels was proposed to manage numerous antennas. While the communication system may change between frames, it is assumed to remain consistent within each frame. F blocks are used for CE per frame, with the rest for data transmission. Increasing F improves channel prediction but reduces data transfer time. Using A_T antennas, the transmitter approximates the intended wideband mmWave MIMO channel for each block f ($f = 1, 2, \ldots, F$) by using the $A_T \times 1$ training symbols vector $c[f]$. To be clear, we don't consider additive white gaussian noise (AWGN) to be a factor. Therefore, the obtained training signal with a dimension of A_R can be represented.

$$\tilde{d}[f] = \sum_{e=0}^{E-1} G(e)c[f-e] \tag{1}$$

The delay channel E's convolution matrices and matching training vectors are shown; these are represented by the notation $c[f-e] \in C^{A_T \times 1}$. As with (1), this representation is as (2):

$$\tilde{d}[f] = \sum_{e=0}^{E-1} \sum_{h=0}^{A_T} g_h(e)c_h[f-e] \tag{2}$$

The h-th element of the vector $c[f]$ is shown by $c_h[f-e]$, while the h-th column of the matrix $G(r)$ is represented by $g_h(e)$. We can change the order of summation in (2) to describe the inner convolution sum of the $E \times F$ Toeplitz matrix. In specific, the $E \times F$ Toeplitz matrix h is introduced, and its (e,f)-th element is determined by $\left[\widetilde{D}\right]_{e,f} = c_h[f - E - e + 2]$. Where $h = 1, 2, \dots, A_T$ and $e = 0, 1, 2, \dots, E-1$. The expression provided in the preceding (2) can be expressed as (3):

$$\widetilde{D} = \sum_{h=1}^{A_T} \tilde{G}_h \widetilde{\mathrm{M}}_h \tag{3}$$

Where, $\tilde{G}_h = [g_h(0) \dots g_h(E-1)] \in \mathbb{C}^{A_R \times E} and \tilde{Y} \in \mathbb{C}^{A_R \times F}$. The arrangement of $\tilde{\mathrm{M}}$ and $\tilde{\mathrm{G}}$ is revised to be organized according to transmitting antennas, resulting (4) as follows $\widetilde{D} = \tilde{M}\ \tilde{G}$. Where, $\widetilde{\mathrm{M}} = [\mathrm{M}^F(0) \dots \mathrm{M}^F(E-1)]^F \in \mathbb{C}^{EA_T \times F}$ and $\tilde{G} = [G(0) \dots G(E-1)] \in \mathbb{C}^{A_R \times EA_T}$. Furthermore, the decomposition of the beamspace matrix at each delay path is as (4):

$$\bar{G} = N_R \bar{P}(I_R \otimes N_T^G), \widetilde{D} = N_R \bar{P}(I_R \otimes N_T^G)\tilde{M} \tag{4}$$

Where, $\bar{P} = [P(0) \dots P(E-1)] \in \mathbb{C}^{A_R \times EA_T}$. In the scenario of the wideband channel matrix $\bar{\mathrm{G}}$, the decomposition outlined in (4) is equivalent to the beamspace decomposition stated in (4) ($\widetilde{D}$ value). Consolidating all the aforementioned details, the matrix incorporating the received training symbols is presented as $\widetilde{D}$. The difference between ($\bar{G}$) and ($\widetilde{D}$) is that the latter includes the training symbols in the rightmost matrix $\tilde{\mathrm{M}}$. The latter formula will be utilized in our method to represent the incoming training data with respect to the combined virtual channel gains $\bar{\mathrm{P}}$.

We provide a thorough analysis of the problem related to the suggested CE procedure as well as a thorough algorithmic fix, and the summing of the AWGN matrix A and the low-rank matrix. That comprises the learning symbols delivered across the wideband mmWave MIMO link, yields the received learning signal matrix at the extended connector's output. The low-rank property of $\tilde{\mathrm{D}}$ is utilized in this study to estimate the wideband channel matrix $\bar{\mathrm{P}}$. First, for simplicity's sake, we look at the later matrix's rank properties.

We formulate the subsequent dual-purpose optimization procedure for estimating $\bar{\mathrm{P}}$, exploiting on both the sparsity structure of $\bar{\mathrm{P}}$ and low-rank property of the learning symbols' matrix $\tilde{\mathrm{D}}$:

$$min_{D,\bar{P}}\ Q_R \|D\|_* + Q_p \|\bar{P}\|_1 \tag{5}$$

Which subject to, $R_\Omega = \Omega(\mathrm{D} + A), D = U\bar{P}V$. During the optimization process, the low-rank property of D is enforced by the nuclear norm, while the sparsity of $\bar{\mathrm{P}}$ is enforced by the e_1-norm. Usually, one may calculate the positive weighted parameters Q_R and Q_P by considering the number E of distinct propagation paths for mmWave MIMO channels. We replace the initial restriction in (5) with its least-squares approximation $\|R_\Omega - \Omega * \mathrm{D}\|_S^2$ in the following because of the uncertainty in the noisy matrix A.

The optimization problem (5) is effectively solved by using the alternating direction method of multipliers technique. As stated in the mathematical (5), sampling is carried out on the channel matrix relatively than the received signal learning. In order to tackle this optimization issue, the subsequent actions are implemented and to recast the desired procedure into an analogous form, we first introduce two input matrix variables: $Z \in C^{A_R \times F} and\ W = D - U\bar{P}V$.

$$min_{D,\bar{P},Z,W}\ Q_R \|D\|_* + Q_P \|\bar{P}\|_1 + ½\|W\|_S^2 + 1/2\|\Omega * Z - R_\Omega\|_S^2 \tag{6}$$
$$Subject\ to\ D = Z\ and\ W = D - U\bar{P}V$$

In this case, the cost function may be broken down into four variables: $D, P, W, and\ Z$. This is in line with (5). Interestingly, the objective function's third component now takes care of the discretization error, while the fourth term accounts for the interference noise that AWGN introduces. The Lagrangian function optimization procedure is easily represented as (7):

$$\mathcal{L}(D,\bar{P},Z,W,X_1,X_2) = Q_R \|D\|_* + Q_P \|\bar{P}\|_1 + ½\|W\|_S^2 + 1/2\|\Omega * Z - R_\Omega\|_S^2 + \tag{7}$$
$$tr\left(X_1^G(D-Z)\right) + \rho/2\|D - \mathrm{Z}\|_S^2 + tr\left(X_2^G(W - Z + U\bar{P}V)\right) + \rho/2\|W - Z + U\bar{P}V\|_S^2$$

The dual factors in this case are represented by $X_1 \in \mathbb{C}^{A_R \times T}$ and $X_2 \in \mathbb{C}^{A_R \times 1}$, which operate as Lagrange multipliers to add the constraints of (7) to the cost function. The ARSCE step size is indicated by the parameter ρ. According to the typical approach, for each i-th algorithmic step ($i = 0, 1, \dots, I_{max}$ the following separate sub-problems must be solved:

$$X_1^{(i+1)} = X_1^{(i)} + \rho\left(Z^{(i+1)} - D^{(i+1)}\right), X_2^{(i+1)} = X_2^{(i)} + \rho\left(W^{(i+1)} - Z^{(i+1)} - U\bar{P}^{(i+1)}V\right) \qquad (8)$$

Since the first subproblem concerns the optimization of variable D, let's formulate it by concentrating on the relevant terms and streamlining the notation, that is,

$$D^{(i+1)} = arg\ min_D\ Q_D\|D\|_* + \rho/2\ \left\|D - \left(Z^{(i)} - 1/\rho\left(X_1^{(i)}\right)\right)\right\|_S^2 \qquad (9)$$

It is thought that the singular value thresholding (SVT) function can be used to get the following solution to (14) [36].

$$D^{(i+1)} = F_E^{(i)} diag\left(sign\left(K_j^{(i)}\right) \times max\left(K_j^{(i)}, 0\right)_{1 \le j \le r}\right)\left(F_R^{(i)}\right)^G \qquad (10)$$

Here, $K_j^{(i)} = \sigma_j - Q/\rho$, where σ_j represents the r singular values, and $F_R^{(i)}$ and $F_E^{(i)}$ include the right and left singular vectors of matrix $(Z^{(i)} - 1/\rho(X_1^{(i)}))$. Inverting the matrix is necessary to solve this equation, but because of diagonal matrix, the issue that can be solving by the following mathematical model:

$$z = (H_1 + 2\rho I)^{-1}\left(X_1^{(i)} + \rho D^{(i+1)} + R_\Omega + X_2^{(i)} + \rho W^{(i)} + \rho H_2 \bar{P}^{(i)}\right) \qquad (11)$$

In the case of the unknown variable $\bar{\mathrm{P}}$, it can be formulated as the vectorization-based minimization of $\bar{\mathrm{P}}$, much like the corresponding sparse optimization issue. In order to address this problem, we use the traditional LASSO form [37], that is $min_{\bar{P}}\ \|\bar{P}\|_1 + \|\bar{P} - Y^{(i)}\|_2^2$. Here, $\bar{p}$ can be approximated using a soft-thresholding function and $Y^{(i)} \in \mathbb{C}^{E A_T A_R \times 1}$, as (12):

$$\bar{p}^{(i+1)} = sign\left(R\left(Y^{(i)}\right)\right)°max\left(\left|R\left(Y^{(i)}\right)\right| - Q_P', 0\right) + sign\left(Img\left(Y^{(i)}\right)\right)°max\left(\left|Img\left(Y^{(i)}\right)\right| - Q_P', 0\right) \qquad (12)$$

In this case, $Q_P' = QP/\rho$, and the $sign(.)$ and $max(.)$ operations are applied component-wise. Significantly, the suggested evolutionary algorithm will make use of the superscript $(i + 1)$. The vector obtained from (12) is then parametrically generated as follows: $\bar{P}^{(i+1)} \in \mathbb{C}^{E A_T \times A_R}$.

The increasing of computational complexity has served the major challenge in the proposed model, so to overcome the computation burden for the $\gamma^{(i)}$, which is written by $\gamma^{(i)} \triangleq H_2^\dagger h^{(i)} \in \mathbb{C}^{A_R A_T \times 1}$. The normal form of the equation as $\varpi\gamma^{(i)} \triangleq v^{(i)}$. Where the ϖ and $v^{(i)}$ can be formulated as (13):

$$\varpi \triangleq H_2^G H_2 \in \mathbb{C}^{E A_R A_T \times E A_R A_T}, v^{(i)} \triangleq H_2^G h^{(i)} \in \mathbb{C}^{E A_R A_T \times 1} \qquad (13)$$

In order to calculate error at every iteration i, the exact least-square method was getting used in ARSCE. Here, we approximate $\gamma^{(i)}$ using the GD optimization and the (i)th iteration can be given as (14):

$$\tilde{\gamma}^{(i)} = \tilde{\gamma}^{(i-1)} - \varphi^{(i)}\beta^{(i)}, \beta^{(i)} = v^{(i)} - \varpi\tilde{\gamma}^{(i-1)} \qquad (14)$$

Here, $\beta^{(i)}$ denotes the residual of $(i) - th$ iteration. To approximate $\beta^{(i)}$ the over variation of i iteration, each step is varying at the right-hand side and $\varphi^{(i)}$ denotes the step size. The $\varphi^{(i)}$ can be computed by a pre-fixed value, i.e., $\beta^{(i)}$ is always be greater to zero.

$$\varphi^{(i)} = \left(\beta^{(i)}\right)^G \beta^{(i)} / \left(\beta^{(i)}\right)^G U\beta^{(i)} \qquad (15)$$

The eigenvalue can be computed using the ratio of largest to smallest; $\varepsilon \triangleq \mu_{max}/\mu_{min}$. The spectral variation of the matrix ϖ totally depends upon the convergence proportion of GD optimization approach and called as eigenvalue. Moreover, the upper bound for the i-step residual computation is written as (16):

$$\left\|\kappa^{(i)}\right\|U \le \left(\frac{\varepsilon-1}{\varepsilon+1}\right)\left\|\kappa^{(0)}\right\|U \qquad (16)$$

The $\kappa^{(i)}$ denotes the residual vector and ϖ is the diagonal leading matrix, which insure the spread of the constraint eigenvalue and the fast convergence rate; $\kappa^{(i)} \triangleq \gamma^{(opt)} - \gamma^{(i)}$. In terms of computational

efficiency, our approach requires only two matrix-vector products to get the GD step size and residual, as opposed to computing the pseudoinverse of H_2. While the modified GD technique presented here yields an approximate answer, its performance is favorable. This is due to a notable property of ARSCE, which states that convergence can be seen in some situations where the alternating minimalization stages are performed rather imprecisely.

The proposed ASACE model, featuring random spatial sampling and an analogue combiner, improves CE by randomly selecting analogue receive beams during the channel period. This enhances the efficiency of gathering channel session measurements, leading to better accuracy in estimating CSI. Coupled with the CSI estimation approach, the ASACE model reduces the training periods needed for CE. Utilizing the low-rank property of channel matrix and received signal matrix at training phase in the beamspace, the model systematically estimates channel characteristics. Additionally, the low-rank charaterstics of narrowband mmWave MIMO channels aids measurement requirements and scalability for wideband channels. Incorporating GD optimization reduces residual errors and computational complexity, making the approach feasible for practical systems with limited computational resources.

4. RESULTS AND DISCUSSION

In this section, we will examine the use of mmWave MIMO technology with considering a large range of A_R and A_T. Using the adaptive random spatial combining design, the performance of the suggested wideband CE method for HBF transmission is assessed. With MATLAB, all computational simulations are carried out. In particular, we average findings from several Monte-Carlo realizations to approximate average mean square error (MSE) performances. Furthermore, we compare the computational cost and convergence rate of the suggested method to comparable state-of-the-art techniques.

SVT [36] is employed in this strategy to solve the rank-constrained optimization problem. orthogonal matching pursuit (OMP) [38] is one example of an iterative thresholding technique that can effectively handle L1 minimization with little computational burden, although its estimation accuracy is best suited for highly sparse vectors, or situations where the unknown vector has few non-zero members. On the other hand, more reliable estimation performance is provided by message passing methods such as vector-AMP (VAMP) [39], particularly for signals with reduced sparsity and measurements that are prone to higher noise levels. These accepted practices are taken into account to contrast with the suggested strategy. Vadgave *et al*. [40], proposed ARSCE is the approach which not taking the training advantage using the GD, therefore we have considered this approach to validate our proposed model.

The system comprises 16 transmitting antennas, 32 receiving antennas, a total of 4 clusters, 6 channel realizations, 4 receive RF chains, a variable number of training frames ranging from 5 to 40, and operates under a signal-to-noise ratio (SNR) of -15 dB with 20 algorithmic iterations. The result analysis based on the provided Figure 1 for frames length vs normalized mean square error (NMSE) (error), with ASACE as the proposed approach; frames length 5: ASACE improves over SVT, OMP and ARSCE by 37.92%, 24.41%, and 26.08%. Frames length 25: ASACE improves over SVT, OMP and ARSCE by 63.58%, 35.09%, and 50.83%. Frames length 40: ASACE improves over SVT, OMP, and ARSCE by 59.91%, 39.38%, and 17.05%. These percentages indicate the reduction in NMSE achieved by ASACE compared to each alternative approach, higher positive values indicate a more significant improvement. In all cases, ASACE demonstrates substantial improvement over SVT, OMP, and ARSCE, showcasing its effectiveness in enhancing the estimation accuracy for different frame lengths.
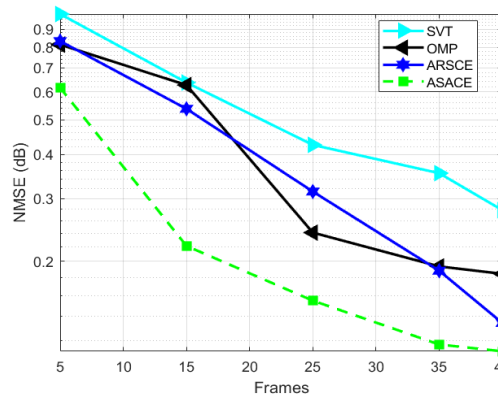

Figure 1. Frames length vs NMSE

The specifications for Figure 2 include 16 transmitting antennas, 32 receiving antennas, a total of 4 clusters, 6 channel realizations, 16 receive RF chains, 5 training frames, and -5 dB SNR with 20 algorithmic iterations. Figure 3 illustrates the efficacy of the proposed CE approach in terms of NMSE against the number of RF chains. ASACE consistently outperforms the other methods, showing improvements ranging from 22.64% to 27.47% at increasing number of RF chains.

Details for Figure 3 include 16 transmitting antennas, 32 receiving antennas, 48 channel propagation paths, 4 total clusters, 1 channel realization, 4 receive RF chains, 30 training frames, and -5 SNR with 10 algorithmic iterations. The figure displays the NMSE concerning the number of channel paths. In this analysis, ASACE consistently demonstrates superior performance compared to other methods, showcasing improvements ranging from 15.21% to 21.59% as the number of channel paths increases. Examined parameter specifications for Figure 4; include 16 transmitting antennas, 32 receiving antennas, 12 channel propagation paths, a total of 4 clusters, channel realization set at 6, 4 receive RF chains, 25 training frames, and an SNR of -10, with 10 iterations in the algorithmic process. Table 1 shows the numerical representation of number of channel delay taps vs NMSE for the better understanding of Figure 4. In Figure 5, the specific parameters include 4 transmitting antennas, 32 receiving antennas, a total of 4 clusters, 100 channel realizations, 4 receive RF chains, 35 training frames, and an SNR range from -15 to 15, with 100 algorithmic iterations.
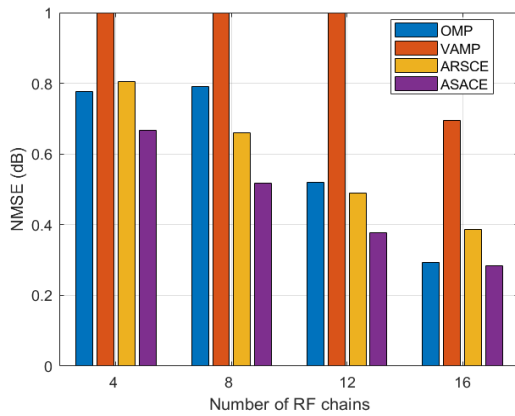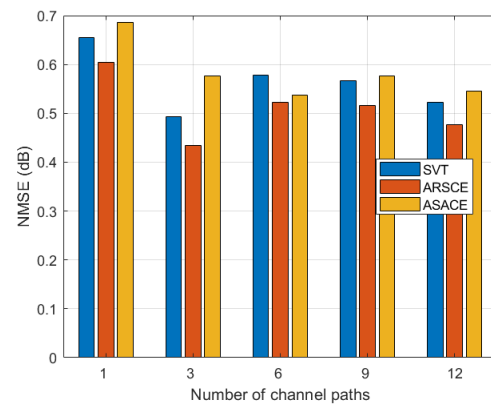

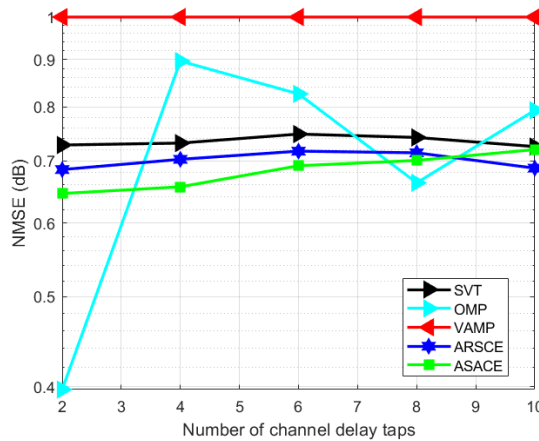Figure 2. RF chains vs NMSE

Figure 3. Channel paths vs NMSE

Figure 4. No. of channel delay taps vs NMSE

Table 1. Numerical representation of no. of channel delay taps vs NMSE

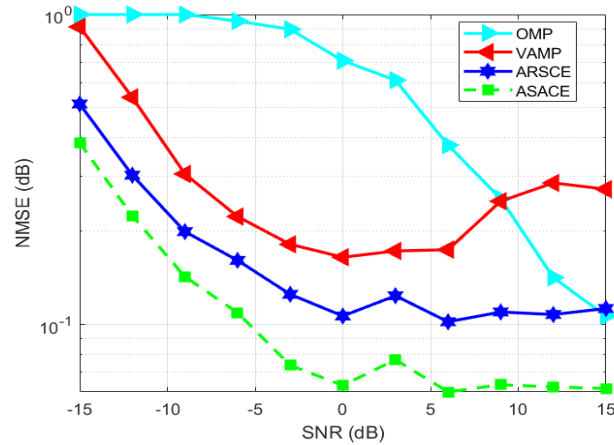| No. of channel delay taps	SVT	OMP	VAMP	ARSCE	ASACE
2	0.72829	0.39737	1	0.68528	0.64581
4	0.73175	0.89659	1	0.70293	0.65666
6	0.74829	0.82667	1	0.71729	0.69182
8	0.74204	0.66316	1	0.71437	0.70101
10	0.72545	0.79379	1	0.68766	0.72010

Figure 5. SNR vs NMSE

The NMSE efficacy is depicted in Figure 5, illustrating its variation with different SNR. In this analysis, ASACE consistently showcase the superior performance as related to other considered methods. Table 2 shows the numerical representation of SNR vs NMSE for the better understanding of Figure 5 and it showcasing all the numerical variation through out the SNR values.

Table 2. Numerical representation of SNR vs NMSE

SNR	OMP	VAMP	ARSCE	ASACE
-15	1	0.912329542	0.514239731	0.385363559
-12	1	0.540224532	0.303055818	0.224176123
-9	1	0.305913199	0.199276421	0.142559385
-6	0.952277289	0.222858988	0.16096364	0.109106506
-3	0.895688663	0.181333251	0.12508141	0.073796403
0	0.709409506	0.164766657	0.106445753	0.063582378
3	0.613868381	0.17258491	0.123746377	0.076949825
6	0.378957823	0.174220045	0.101970491	0.060589505
9	0.254511226	0.249832965	0.10966335	0.063881907
12	0.141629256	0.286092178	0.107637722	0.06283538
15	0.106478596	0.27317278	0.112553388	0.062141885

5. CONCLUSION

This paper presents the ASACE technique for wideband mmWave MIMO CE, leveraging the channel's low-rank properties and beamspace sparsity for enhanced accuracy, particularly in short beam learning intervals. The low-rank matrix sum, incorporating learned signals through the system, is represented by the received matrix of training signal at the extended link's end. GD optimization further refines the approach, reducing residual errors and computational complexity. Simulation results showcase improved performance in NMSE, especially in short beam training and noisy environments. Comparative analysis highlights the ARSCE model's superior channel estimates, translating to higher throughput and enhanced user experience. This study signify a significant advancement in wideband mmWave MIMO CE techniques, offering improved accuracy and efficiency, particularly in challenging environments with short beam training durations. Moreover, this contributes to the ongoing efforts to enhance wireless communication systems, benefiting various sectors and applications within the research community and broader society. Future research can explore extensions of ASACE to address specific challenges such as dynamic channel conditions, mobility scenarios, and diverse antenna configurations. Additionally, investigations into the integration of machine learning techniques for enhanced CE could be pursued.

REFERENCES

[1] T. S. Rappaport *et al*., "Millimeter Wave Mobile Communications for 5G Cellular: It Will Work!," in *IEEE Access*, vol. 1, pp. 335-349, 2013, doi: 10.1109/ACCESS.2013.2260813.
[2] T. S. Rappaport *et al*., "Wireless Communications and Applications Above 100 GHz: Opportunities and Challenges for 6G and Beyond," in *IEEE Access*, vol. 7, pp. 78729-78757, 2019, doi: 10.1109/ACCESS.2019.2921522.

[3]   H. Elayan, O. Amin, B. Shihada, R. M. Shubair, and M. -S. Alouini, "Terahertz Band: The Last Piece of RF Spectrum Puzzle for Communication Systems," in *IEEE Open Journal of the Communications Society*, vol. 1, pp. 1-32, 2020, doi: 10.1109/OJCOMS.2019.2953633.

[4]   Y. -W. Wu, Z. -C. Hao, and Z. -W. Miao, "A Planar W-Band Large-Scale High-Gain Substrate-Integrated Waveguide Slot Array," in *IEEE Transactions on Antennas and Propagation*, vol. 68, no. 8, pp. 6429-6434, Aug. 2020, doi: 10.1109/TAP.2020.2969999.

[5]   L. Dai, B. Wang, M. Peng, and S. Chen, "Hybrid Precoding-Based Millimeter-Wave Massive MIMO-NOMA With Simultaneous Wireless Information and Power Transfer," in *IEEE Journal on Selected Areas in Communications*, vol. 37, no. 1, pp. 131-141, Jan. 2019, doi: 10.1109/JSAC.2018.2872364.

[6]   B. Ning *et al.*, "Prospective beamforming technologies for ultra-massive MIMO in terahertz communications: A tutorial," *arXiv*, 2021, doi: 10.48550/arXiv.2107.03032.

[7]   R. Dogra, S. Rani, H. Babbar, and D. Krah, "Energy-efficient routing protocol for next-generation application in the Internet of Things and wireless sensor networks," *Wireless Communications and Mobile Computing*, vol. 2022, pp. 1–10, Mar. 2022, doi: 10.1155/2022/8006751.

[8]   H. L. Gururaj, R. Natarajan, N. A. Almujally, F. Flammini, S. Krishna, and S. K. Gupta, "Collaborative Energy-Efficient Routing Protocol for Sustainable Communication in 5G/6G Wireless Sensor Networks," in *IEEE Open Journal of the Communications Society*, vol. 4, pp. 2050-2061, 2023, doi: 10.1109/OJCOMS.2023.3312155.

[9]   H. F. Schepker and A. Dekorsy, "Compressive Sensing Multi-User Detection with Block-Wise Orthogonal Least Squares," *2012 IEEE 75th Vehicular Technology Conference (VTC Spring)*, Yokohama, Japan, 2012, pp. 1-5, doi: 10.1109/VETECS.2012.6240301.

[10]   X. Xu, X. Rao and V. K. N. Lau, "Active user detection and channel estimation in uplink CRAN systems," *2015 IEEE International Conference on Communications (ICC)*, London, UK, 2015, pp. 2727-2732, doi: 10.1109/ICC.2015.7248738.

[11]   G. Wunder, P. Jung, and M. Ramadan, "Compressive Random Access Using a Common Overloaded Control Channel," *2015 IEEE Globecom Workshops (GC Wkshps)*, San Diego, CA, USA, 2015, pp. 1-6, doi: 10.1109/GLOCOMW.2015.7414186.

[12]   G. Hannak, M. Mayer, A. Jung, G. Matz, and N. Goertz, "Joint channel estimation and activity detection for multiuser communication systems," *2015 IEEE International Conference on Communication Workshop (ICCW)*, London, UK, 2015, pp. 2086-2091, doi: 10.1109/ICCW.2015.7247489.

[13]   G. Wunder, H. Boche, T. Strohmer, and P. Jung, "Sparse Signal Processing Concepts for Efficient 5G System Design," *in IEEE Access*, vol. 3, pp. 195-208, 2015, doi: 10.1109/ACCESS.2015.2407194.

[14]   Z. Chen and W. Yu, "Massive device activity detection by approximate message passing," *2017 IEEE International Conference on Acoustics, Speech and Signal Processing (ICASSP)*, New Orleans, LA, USA, 2017, pp. 3514-3518, doi: 10.1109/ICASSP.2017.7952810.

[15]   Z. Chen, F. Sohrabi, and W. Yu, "Sparse Activity Detection for Massive Connectivity," in *IEEE Transactions on Signal Processing*, vol. 66, no. 7, pp. 1890-1904, 1 April1, 2018, doi: 10.1109/TSP.2018.2795540.

[16]   M. Bayati and A. Montanari, "The Dynamics of Message Passing on Dense Graphs, with Applications to Compressed Sensing," in *IEEE Transactions on Information Theory*, vol. 57, no. 2, pp. 764-785, Feb. 2011, doi: 10.1109/TIT.2010.2094817.

[17]   X. Zhang, S. Sun, M. Tao, Q. Huang and X. Tang, "Joint Hybrid Beamforming and User Scheduling for Multi-Satellite Cooperative Networks," *2023 IEEE Wireless Communications and Networking Conference (WCNC)*, Glasgow, United Kingdom, 2023, pp. 1-6, doi: 10.1109/WCNC55385.2023.10118769.

[18]   J. W. Choi, B. Shim, Y. Ding, B. Rao, and D. I. Kim, "Compressed Sensing for Wireless Communications: Useful Tips and Tricks," in *IEEE Communications Surveys & Tutorials*, vol. 19, no. 3, pp. 1527-1550, thirdquarter 2017, doi: 10.1109/COMST.2017.2664421.

[19]   K. Dovelos, M. Matthaiou, H. Q. Ngo, and B. Bellalta, "Channel Estimation and Hybrid Combining for Wideband Terahertz Massive MIMO Systems," in *IEEE Journal on Selected Areas in Communications*, vol. 39, no. 6, pp. 1604-1620, Jun. 2021, doi: 10.1109/JSAC.2021.3071851.

[20]   M. Cui and L. Dai, "Channel Estimation for Extremely Large-Scale MIMO: Far-Field or Near-Field?," in *IEEE Transactions on Communications*, vol. 70, no. 4, pp. 2663-2677, Apr. 2022, doi: 10.1109/TCOMM.2022.3146400.

[21]   X. Wei and L. Dai, "Channel Estimation for Extremely Large-Scale Massive MIMO: Far-Field, Near-Field, or Hybrid-Field?," in *IEEE Communications Letters*, vol. 26, no. 1, pp. 177-181, Jan. 2022, doi: 10.1109/LCOMM.2021.3124927.

[22]   Y. Ding and B. D. Rao, "Dictionary Learning-Based Sparse Channel Representation and Estimation for FDD Massive MIMO Systems," in *IEEE Transactions on Wireless Communications*, vol. 17, no. 8, pp. 5437-5451, Aug. 2018, doi: 10.1109/TWC.2018.2843786.

[23]   J. Ma and L. Ping, "Orthogonal AMP," in *IEEE Access*, vol. 5, pp. 2020-2033, 2017, doi: 10.1109/ACCESS.2017.2653119.

[24]   S. Srivastava, A. Tripathi, N. Varshney, A. K. Jagannatham and L. Hanzo, "Hybrid Transceiver Design for Tera-Hertz MIMO Systems Relying on Bayesian Learning Aided Sparse Channel Estimation," in *IEEE Transactions on Wireless Communications*, vol. 22, no. 4, pp. 2231-2245, Apr. 2023, doi: 10.1109/TWC.2022.3210306.

[25]   R. Wang, H. He, S. Jin, X. Wang, and X. Hou, "Channel Estimation for Millimeter Wave Massive MIMO Systems with Low-Resolution ADCs," *2019 IEEE 20th International Workshop on Signal Processing Advances in Wireless Communications (SPAWC)*, Cannes, France, 2019, pp. 1-5, doi: 10.1109/SPAWC.2019.8815551.

[26]   C. Huang, L. Liu, C. Yuen, and S. Sun, "Iterative Channel Estimation Using LSE and Sparse Message Passing for MmWave MIMO Systems," in *IEEE Transactions on Signal Processing*, vol. 67, no. 1, pp. 245-259, Jan. 2019, doi: 10.1109/TSP.2018.2879620.

[27]   A. Liu, L. Lian, V. K. N. Lau, and X. Yuan, "Downlink Channel Estimation in Multiuser Massive MIMO With Hidden Markovian Sparsity," in *IEEE Transactions on Signal Processing*, vol. 66, no. 18, pp. 4796-4810, Sep. 2018, doi: 10.1109/TSP.2018.2862420.

[28]   G. Arya, A. Bagwari, and D. S. Chauhan, "Performance Analysis of Deep Learning-Based Routing Protocol for an Efficient Data Transmission in 5G WSN Communication," in *IEEE Access*, vol. 10, pp. 9340-9356, 2022, doi: 10.1109/ACCESS.2022.3142082.

[29]   S. U. Rehma, A. Hussain, F. Hussain, and M. A. Mannan, "A comprehensive study: 5G wireless networks and emerging technologies," *5 th International Electrical Engineering Conference (IEEC 2020)*, vol. 5, pp. 25–32, Feb. 2022.

[30]   K. Q. Vu, V. K. Solanki, and A.-N. Le, "A saving energy MANET routing protocol in 5G," in *Secure Communication for 5G and IoT Networks. Cham*, Switzerland: Springer, 2022.

[31]   M. Mir and M. Khairabad, "A new approach to energy-aware routing in the Internet of Things using improved grasshopper metaheuristic algorithm with Chaos theory and fuzzy logic," *Multimedia Tools and Applications*, vol. 82, pp. 5133–5159, Feb. 2023, doi: 10.1007/s11042-021-11841-9.

[32] R. Nithya *et al*., "An optimized fuzzy based ant colony algorithm for 5G-MANET," *Computers, Materials & Continua*, vol. 70, no. 1, pp. 1069–1087, May 2021, doi: 10.32604/cmc.2022.019221.

[33] M.-K. Wong, C.-L. Hsu, T.-V. Le, M.-C. Hsieh, and T.-W. Lin, "Three-factor fast authentication scheme with time bound and user anonymity for multi-server E-health systems in 5G-based wireless sensor networks," *Sensors*, vol. 20, no. 9, p. 2511, 2022, doi: 10.3390/s20092511.

[34] M. K. Chary, C. H. V. Krishna, D. R. Krishna, "Accurate channel estimation and hybrid beamforming using Artificial Intelligence for massive MIMO 5G systems," *AEU - International Journal of Electronics and Communications,* vol. 173, p. 154971, 2024, doi: 10.1016/j.aeue.2023.154971.

[35] A. F. Molisch *et al*., "Hybrid Beamforming for Massive MIMO: A Survey," in *IEEE Communications Magazine*, vol. 55, no. 9, pp. 134-141, Sept. 2017, doi: 10.1109/MCOM.2017.1600400.

[36] J. F. Cai, E. J. Candes, and Z. Shen, "A singular value thresholding ` algorithm for matrix completion," *SIAM Journal on Optimization*, vol. 20, no. 4, pp. 1956–1982, 2010, doi: 10.1137/080738970.

[37] R. Tibshirani, "Regression shrinkage and selection via the Lasso*," Journal of the Royal Statistical Society: Series B (Methodological)*, vol. 58, 1, pp. 267–288, 1996, doi: 10.1111/j.2517-6161.1996.tb02080.x.

[38] K. Venugopal, A. Alkhateeb, N. G. Prelcic, and R. W. Heath, "Channel Estimation for Hybrid Architecture-Based Wideband Millimeter Wave Systems," in *IEEE Journal on Selected Areas in Communications*, vol. 35, no. 9, pp. 1996-2009, Sept. 2017, doi: 10.1109/JSAC.2017.2720856.

[39] P. Schniter, S. Rangan and A. K. Fletcher, "Vector approximate message passing for the generalized linear model," *2016 50th Asilomar Conference on Signals, Systems and Computers, Pacific Grove*, CA, USA, 2016, pp. 1525-1529, doi: 10.1109/ACSSC.2016.7869633.

[40] R. M Vadgave, M. S., and T. S. Vishwanath "Adaptive Random Spatial Based Channel Estimation (ARSCE) For Millimeter Wave MIMO System," *International Journal of Computer Networks & Communications (IJCNC)*, vol. 14, no. 1, pp. 85-98, 2022.

BIOGRAPHIES OF AUTHORS

Rajkumar M. Vadgave received the B.E. in Electronics and Communication Engineering from VTU Belagavi University in 2011 and M.Tech. in Communication Systems from VTU Belagavi University in 2013. He is pursuing Ph.D. from VTU Belagavi University. He is currently working as assistant professor in the Department of Electronics and Communication Engineering, Bheemanna Khandre Institute of Technology, Bhalki, India. He has Authored or Coauthored more than 6 referred journals and conference papers. His research interest includes wireless sensor network and communication system. He can be contacted at email: rajkumarv074@gmail.com.

Manjula S. received the BE in Electronics and Communication Engineering from Gulbarga University in 1997 and M.Tech. in Electronics and Communication Engineering from RVD University in 2006 and Ph.D. degree from Singhania University in 2014. She became assistant professor in 1998, an associate professor in 2007 and professor Department of Electronics and Communication Engineering in 2014. She is currently working as professor in the Department of Electronics and Communication Engineering, Bheemanna Khandre Institute of Technology, Bhalki, India. She has authored or coauthored more than 20 referred journals and conference papers. Her research interest includes synthesis characterization and microwave properties of conducting polymer composites. Member of ISTE and IETE. She can be contacted at email: manjulasidramshetty@gmail.com.